

# Inverted pyramid structures fabricated on monocrystalline silicon surface with a NaOH solution

Chenliang Huo<sup>a</sup>, Haoxin Fu<sup>b</sup>, Kui-Qing Peng<sup>a,\*</sup>

<sup>a</sup> College of Education for the Future, Beijing Normal University at Zhuhai, Department of Physics and Beijing Key Laboratory of Energy Conversion and Storage Materials, Beijing Normal University, Beijing, China

<sup>b</sup> Tongwei Solar Company, Chengdu, China

## ARTICLE INFO

### Keywords:

Monocrystalline silicon  
Alkaline etching  
Inverted pyramid  
Solar cell

## ABSTRACT

Low-cost aqueous alkaline etching has been widely adopted for monocrystalline silicon surface texturing in current industrial silicon solar cells. However, conventional alkaline etching can only prepare upright pyramid structures on mono-crystalline silicon surfaces. This study demonstrates for the first time the use of ethylene glycol butyl ether (EGBE) to regulate aqueous anisotropic alkaline etching and prepare inverted pyramid structures on monocrystalline silicon surfaces. Acidic metal-catalyzed etching solutions are not the best choice for monocrystalline silicon due to their inherent disadvantages, such as noble metal pollution and relatively high costs. The one-step method to produce the inverted pyramid structures by using alkaline etch with EGBE additive is simple and inexpensive, does not generate noble metal pollution, and especially compatible with current industrial silicon solar cell production lines. With the use of a sodium hydroxide (NaOH) solution containing a low-cost additive, inverted pyramid structures can be prepared on monocrystalline silicon surface in a short time. This method is suitable for various types of silicon wafers and has great potential for industrial solar cell applications.

## 1. Introduction

In the past decades, silicon, which have many extremely advantageous properties such as chemical stability, high carrier mobility, and nontoxicity, have become the most important materials in the microelectronic and photovoltaic industries and are widely used in biosensors, genetic engineering, electronic devices, photonics devices, and energy technology [1–5]. The technologies used to prepare the micro/nanostructures on silicon surface have always been the focus of researchers. Scientists have conducted various studies on solar cells to improve their photoelectric conversion efficiencies, and surface texturing is one of the critical technologies for improving cell efficiency [6–10]. The conventional flat silicon surface has a high natural reflectivity. The average reflectivity of the flat silicon surface was around 40 % [11]. Surface texturing refers to forming surface microstructures with different shapes on the silicon surface through various techniques to increase light absorption capability. Many texturization methods have been proposed including dry etching techniques such as plasma etching and aqueous wet techniques that involve chemical reactions in solutions [12–14]. Compared to dry etching process, wet etching of crystalline silicon has been studied extensively and used widely in industry due to its low cost and suitability. Aqueous alkaline etching has been widely used in industrial production to form pyramid structures in mono-crystalline silicon solar cells [15]. Pyramid structures can efficiently reduce the surface reflectance by extending the paths of

\* Corresponding author.

E-mail address: [kq\\_peng@bnu.edu.cn](mailto:kq_peng@bnu.edu.cn) (K.-Q. Peng).

<https://doi.org/10.1016/j.heliyon.2023.e23871>

Received 6 August 2023; Received in revised form 23 October 2023; Accepted 14 December 2023

Available online 19 December 2023

2405-8440/© 2023 Published by Elsevier Ltd.

(<http://creativecommons.org/licenses/by-nc-nd/4.0/>).

This is an open access article under the CC BY-NC-ND license

incident photons. In the current production of monocrystalline silicon solar cells, alkaline etching has become the most widely used method for silicon surface texturization due to its low cost and environmental friendliness [16].

The history of alkaline etching of monocrystalline silicon can be traced back to the 1950s when Bell Labs used a KOH and ethanol aqueous solution to perform anisotropic etching of silicon [17]. Seidel et al. [18,19] systematically investigated the effects of different alkaline solutions (such as KOH and NaOH), silicon doping types and concentrations on alkaline etching. Alkaline etching solutions can be roughly categorized into two types. The first type is alkaline solutions containing alcohol additives, typically including alkaline solutions with isopropanol or ethanol. The second type is alkaline solutions without alcohol additives, which are currently the most used in current silicon PV industries. Researchers have realized the drawbacks of isopropanol and conducted extensive studies on alcohol-free additives. Substitutes for isopropanol include tetramethylammonium hydroxide, sodium carbonate, sodium acetate, sodium phosphate, as well as the addition of defoamers or antifoaming agents. However, the present adopted alkaline etching methods only produce upright pyramids on the surface of silicon wafer [20–25]. In 1989, M. A. Green [26] proposed the PERC cell with an efficiency of 22.8 %. The light capture structure in Green's PERC cell was inverted pyramids prepared by KOH etching and photolithography. In 1990, M. A. Green [27] further improved the efficiency to 24 % by locally diffusing boron into the back contact area. In 1999, to reduce the current crowding effect and improve the fill factor, Zhao [28] proposed the PERT cell, which uses localized doping on the back surface to form an efficient *P-N* junction to increase the carrier mobility and improve the efficiency. In 2009, the efficiencies of crystalline silicon solar cells achieved a historic breakthrough, and the efficiencies of PERL cells reached 25 % [29]. Although the PERx series of cells exhibited high efficiencies, the inverted pyramids were prepared by dry etching, which is expensive and cannot be applied widely. Traditional inverted pyramid alkaline texturization techniques require the assistance of technologies such as photolithography or metal-catalyzed etching [30–33], which are incompatible with current monocrystalline silicon texturization production lines. Currently, two methods are typically used for preparing inverted pyramid structures with alkaline solutions: one involves the use of photolithography masks, and the other uses the alkaline etching process after acidic etching [34]. The photolithography mask method uses a material that is not etched by alkaline solutions. First, the material is coated on the silicon wafer surface to form a template shape, and then the silicon wafer is placed in an alkaline solution for etching so that the silicon is etched along the crystal orientation to generate inverted pyramid structures. However, this method has a serious cost disadvantage and requires expensive equipment [9]. The method of alkaline etching after acidic etching also utilizes anisotropic etching methods. Some researchers combined metal-catalyzed etching of silicon with alkaline etching to prepare inverted pyramids on the surface of monocrystalline silicon. First, the silicon wafer surface was converted into a porous structure with a mixed solution containing silver particles or copper ions in hydrofluoric acid-nitric acid, and then the silicon wafer was immersed in a solution containing NaOH, which produced a square inverted pyramid structure. In 2006, Tsujino et al. [35] reported a texturing process for polycrystalline silicon wafers that used platinum and silver particle-assisted chemical etching in an HF solution containing an oxidizing agent. They first used an acid solution to etch holes on the silicon surface and then used an alkaline solution to etch the holes into inverted pyramid structures. In 2014, Ye et al. [36] repeated Tsujino's work and manufactured a class of pyramid-textured slurry line saw-cut polycrystalline silicon solar cells exhibiting efficiencies of up to 18.45 % by using silver-catalyzed etching and alkaline etching. In 2015, Lin et al. [37] prepared nanostructured polycrystalline silicon with controllable geometric shapes and surface areas by Ag-catalyzed etching and subsequent NaOH treatment. They demonstrated a large nanostructured polycrystalline silicon solar cell with a certified efficiency of 17.75 %, which was approximately 0.3 % higher than those of similar acid textured products. In 2018, Xu et al. [38] prepared inverted nanopyramids on a monocrystal silicon wafer by Ag-catalyzed etching and alkaline etching. By optimizing the cell design, they obtained a black silicon solar cell with an efficiency of 20.5 % via nano inverted pyramid texturing. Although inverted pyramid structures have been prepared by alkaline etching, the process is complex and not conducive for large-scale application.

This paper describes a new method for alkaline etching inverted pyramid texturization with industrial prospects. This study has made breakthroughs in regulating anisotropic etching of monocrystalline silicon by alkaline solutions and shows for the first time that an additive (ethylene glycol butyl ether) forms alkali-resistant masks on the surfaces of monocrystalline silicon, which selectively etches polished silicon and monocrystalline silicon slices cut with a diamond wire to form inverted pyramid textures in alkaline solutions. This one-step inverted pyramid texturization method is simple, efficient, and compatible with current industrial monocrystalline silicon alkaline texturization production lines. Using this alkaline etching method, we have tried to fabricate monocrystalline silicon solar cells with inverted pyramid structures. The fabricated cells exhibit low reflection properties, with an efficiency of up to 21.54 %.

## 2. Experimental details

Tables 1 and 2 are all the experimental etching parameters.

**Table 1**  
Texture fabrication.

Cleaning and Etching Process	Details
Degreasing	Sequential ultrasonic cleaning in acetone and ethanol for 5–10 min
Washing	Rinse with deionized (DI) water for 10 min
Acid Cleaning	Clean in acid solution [ $\text{H}_2\text{SO}_4$ (98 %): $\text{H}_2\text{O}_2$ (30 %) = 3:1] for 10–20 min
Rinsing	Thorough rinse with excess DI water
Oxide Removal	Dip in dilute HF solution for 1 min to remove surface oxides
Etching Setup	Introduction of cleaned wafers into PTFE vessels filled with NaOH and EGBE
Heating	Heat at 80 °C for desired time
NaOH Concentration	Controlled within mass fraction range of 1%–10 %
EGBE Amount	Optimal amount used: 40–45 mL
Etching Time	20 min
Etching Solution Volume	50 mL
Experimental Temperature	355 K
Rinse and Drying	Copious rinse with DI water and dry with ultrapure nitrogen gas or air-dry at room temperature

Note:Silicon wafers used were p-type (B doped, 15–25  $\Omega\bullet\text{cm}$ , (100)).

**Table 2**  
Characterization and measurement equipment.

Characterization	Measurement Equipment
Morphological Analysis	High-resolution scanning electron microscopy (Hitachi-SU8010)
Reflectance Measurement	UV–Vis–NIR spectrophotometer (Shimadzu, UV-3600, with an integrating sphere) over the wavelength range 300–1100 nm. Hemispheric total reflectance for normal incidence measured with a Varian Cary 5000 spectrophotometer with an integrating sphere.
Elemental Analysis	Energy Dispersive X-ray Spectroscopy (EDS) using Phenom-ProX-EDS instrument.

2.1. Solar cell fabrication

All textured p-type silicon wafers ( $156.75 \times 156.75 \text{ mm}^2$ ) were loaded into a quartz boat and placed in a tube furnace to form a P–N junction using high-temperature diffusion at 870 °C for 90 min. The source of phosphorus used in the diffusion process was  $\text{POCl}_3$ . Thereafter, these silicon wafers were placed on a conveyor belt, were rinsed in an alkaline solution to make the rear of the silicon smoother, and were placed in hydrofluoric acid with nitric acid to remove the phosphosilicate glass (PSG) at the edges. Then, the wafers were rinsed with deionized water, dried with nitrogen, and put into a graphite boat to deposit an 80-nm-thick silicon nitride layer as an anti-reflection coating on the front surface of the silicon wafer by PECVD for 35 min. Then, we used PECVD to deposit a mixed layer of silicon oxide and silicon nitride on the back of the silicon wafer to perform back passivation for 37 min. A laser instrument was then used to ablate the rear film to achieve rear contact. Electrodes, including silver (Ag) electrodes and aluminum (Al) back fields, were rapidly sintered after being prepared by screen printing technology.

2.2. Materials characterization

The morphologies of the samples were characterized via a high-resolution scanning electron microscope (Hitachi-SU8010). The optical reflectance measurement was performed by a UV–Vis–NIR spectrophotometer (Shimadzu, UV-3600, with an integrating sphere) in the wavelength range of 300–1100 nm. The spectral response characteristics, including IQE (internal quantum efficiency) and EQE (external quantum efficiency), were measured by a spectral response instrument (GP SOLAR, IQE-Scan). The PV cell characteristics were analyzed by hallmark.

3. Results and discussion

Generally, aqueous alkaline etching results in upright pyramids on monocrystalline silicon surface. This was discovered and has been applied since the mid-20th century [17]. The texturization process for monocrystalline silicon wafers involves the anisotropic etching of silicon wafers in an alkaline solution containing either NaOH or potassium hydroxide (KOH). In industrial solar cell production processes, NaOH or KOH are usually chosen due to their lower costs [39,40]. We were inspired to add an additive used in aqueous alkaline etching to assist in the formation of inverted pyramids. After many attempts, we successfully used an alkaline solution with added EGBE to etch inverted pyramid structures on the Si (100) surface. This is the first time that inverted pyramid structures have been prepared in one step in alkaline solutions without photolithography or secondary etching processes but through a one-step wet experimental process, as shown in Fig. 1. Fig. 1 (a)–(d) are the SEM images of the inverted pyramids prepared by a one-step alkaline etching process.

Fig. 2 shows SEM images of the inverted pyramid cross-sections prepared by alkaline texturization. In Fig. 2, a silicon wafer with a long etching time generates large inverted pyramid structures on its surface, which clearly demonstrated the structural characteristics of the inverted pyramids. The oblique 45° SEM image showed that the silicon wafer surface had a very complete and regular inverted pyramid structure, and the edges of the inverted pyramids were clearly visible. The 90° SEM image of the cross-section also shows the

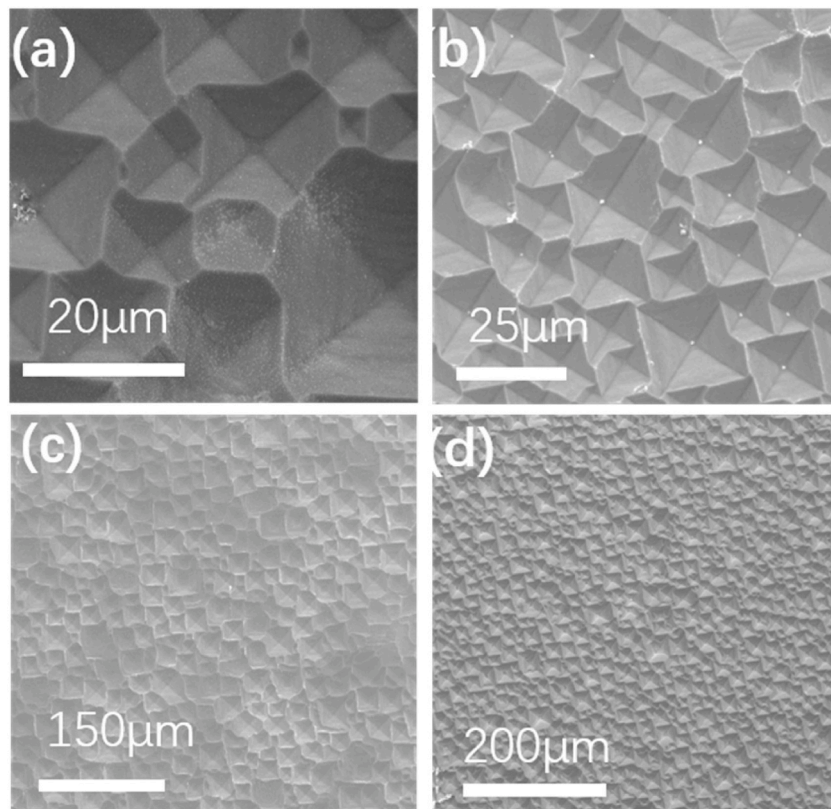


**Fig. 1.** Inverted pyramid SEM images with different magnifications for a p-type silicon wafer (B doped, 15–25  $\Omega\cdot\text{cm}$ , crystal direction (100)) etched with alkaline solution.

downwards concave structure on the silicon wafer surface. Fig. 2(d) demonstrates that an inverted pyramid structure was made with our method.

The main reaction of the monocrystalline silicon in the alkaline solution involved the attack of  $\text{OH}^-$  groups on the silicon-silicon bonds, which caused the silicon atoms to detach from the bulk silicon [18]. Since the bond energies differ for different crystal orientations, there were differences in the reaction rates for the different crystalline orientations, so the alkaline solution etched the silicon surface to form pyramid structures [19]. This paper analyses the formation of inverted pyramid structures in alkaline solutions by characterizing the morphology and elemental content, as shown in Fig. 3. In the experiments, p-type silicon wafers (B-doped, 15–25  $\Omega\cdot\text{cm}$ , oriented (100)) were used, and two variables, the etching time (0.5 h, 1 h) and the EGBE concentration (10 ml, 30 ml, 40 ml, 45 ml), were varied. At low EGBE concentrations, the alkaline solution still etched the silicon wafer and formed upright pyramid structures, as shown in Fig. 3(a) and (e). However, after increasing the EGBE concentration, inverted pyramid structures gradually appeared on the silicon surface, as shown in Fig. 3(b)–(d). Fig. 3(a) and (b) show that the inverted pyramid structure was produced by increasing the EGBE concentration from 10 ml to 30 ml, and the process is similar to those of Fig. 3(e) and (f). The inverted pyramid structure gradually became clearer with increasing EGBE concentration (40 ml, 45 ml), as shown in Fig. 3(c)–(d) and Fig. 3(g)–(h). The SEM images of the upright pyramid structures formed by dilute EGBE in the alkaline solution show that the upright pyramids formed by adding EGBE were no different from those formed by other organic additives, and the sizes of the pyramids were 2–4  $\mu\text{m}$ . In the images of the inverted pyramids formed with higher concentrations of EGBE in alkaline solutions, the sizes of the inverted pyramids gradually increased with increasing EGBE concentration, and the optimum inverted pyramid structure measured approximately 1  $\mu\text{m}$ . According to previous studies, a small size is beneficial for light absorption, and the alkaline solution provides small, inverted pyramids [41,42]. In Fig. 3 (a)–(d), the reaction time was 0.5 h, and the etching times of Fig. 3 (e)–(h) were 1 h. When the etching time and the concentration of EGBE were increased, the inverted pyramids gradually expanded because  $\text{OH}^-$  continued to attack other surfaces of the silicon, which exposed the (100) orientation again. The  $\text{OH}^-$  groups continued to etch the (100) surface rapidly, which eventually led to larger inverted pyramid structures.

In this study, etching was conducted after EDS analyses to determine why the alkaline mixture of EGBE and NaOH produced the inverted pyramid structures. In addition, the alkaline system reacted with silicon and was basically controllable, which is useful in etching large-area silicon wafers [43]. Moreover, for diamond wire-cut silicon wafers, the concentrated NaOH directly removed the cutting line marks so they would not reduce the efficiency of the solar cell. Generally, alkaline etching can be carried out with the following steps: the first step involves rough polishing to remove the damaged layer of the silicon wafer. The second step is fine polishing, which produces a textured surface with a low reflectivity. If (100) crystalline grains exist, pyramid-like textured surfaces can



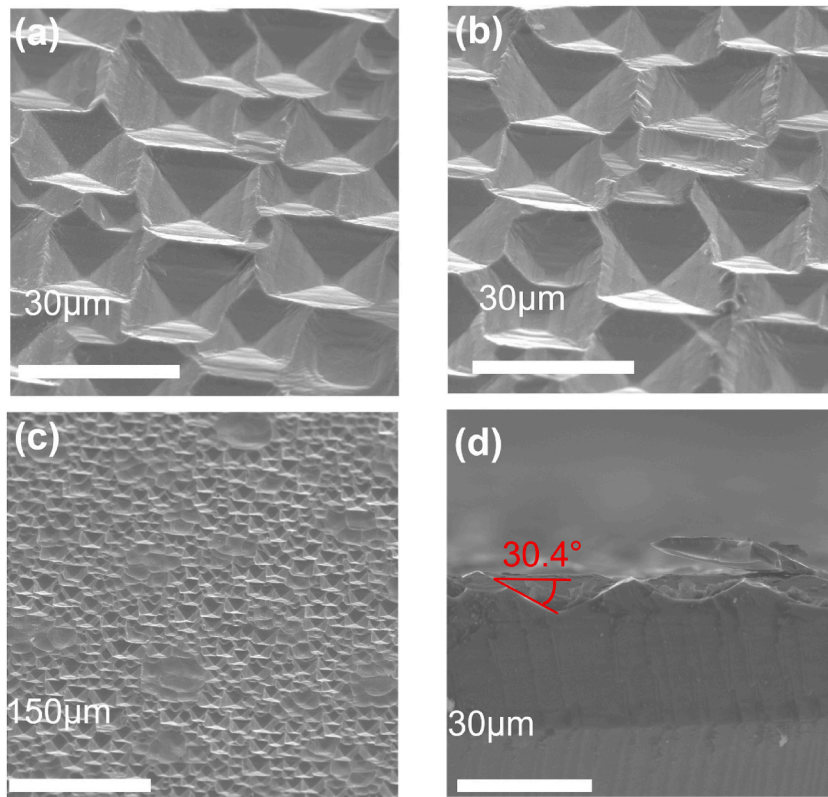


**Fig. 2.** SEM images with different magnifications for inverted pyramid structure sections prepared by etching p-type silicon wafers (B doped, 15–25  $\Omega\cdot\text{cm}$ , crystal direction (100)). (a)–(c) SEM image with a 45° oblique view of silicon. (d) Silicon cross-sectional view shows the texture angle of the inverted pyramids. (For interpretation of the references to colour in this figure legend, the reader is referred to the Web version of this article.)

be grown. Scientists have proposed many explanations for why alkaline solutions etch silicon, and the most convincing model is the electrochemical model proposed by Professor Seidel in 1990 [18,19]. The model suggested that anisotropic etching was fundamentally caused by differences in the densities of dangling bonds and back bonds on the silicon surface.  $\text{OH}^-$  groups can substitute the dangling bonds on the silicon surface and form a silicon hydroxide composite, which then reacts with  $\text{OH}^-$  to generate the original silicic acid. The energy of the silicon (100) crystal orientation is the lowest, and it exhibits the fastest etching and disappearance rates, while the (111) crystal plane is the most difficult to etch, and the exposed (100) surfaces of the silicon wafer eventually show how the upright pyramid structure was produced.

The silicon wafers with inverted pyramid structures used in the EDS analysis were not ultrasonically cleaned, and the EDS results are shown in Fig. 4. The EDS results and SEM images show that there were white substances in the pits after alkaline etching, and the pits were continually etched to form the inverted pyramid structures. The elemental analyses showed that there were several elements present, such as silicon (Si), oxygen (O), and sodium (Na). Fig. 4(a) shows the results of the EDS elemental analyses throughout the region of the image. Fig. 4(b) shows the results of the EDS scans for the elements at cross spot 1 in the image. Based on the mechanism of NaOH etching, it is inferred that the substance was sodium silicate ( $\text{Na}_2\text{SiO}_3$ ). The silicon atoms arose because the white substance formed a thin layer, which caused the substrate silicon to be included in the EDS analysis, so silicon atoms constituted most of the silicon surface content. As shown in Fig. 4(b), due to scanning at a specific spot, Na was more prominently presented, indicating that the surface at this point contained Na, Si, and O. Therefore, we propose the following mechanism for one-step alkaline etching of silicon with EGBE to form inverted pyramid structures: since the  $\text{OH}^-$  groups etched the silicon along the crystal orientation, the silicon was etched along the (100) surface, and the  $\text{Na}_2\text{SiO}_3$  generated during the etching process was insoluble in the EGBE, so only the water in the solution dissolved the  $\text{Na}_2\text{SiO}_3$ . When the solution became saturated, the  $\text{Na}_2\text{SiO}_3$  generated during the etching process was deposited on the silicon surface and acted as a mask. That is, this mechanism was basically the same as the mechanism for preparing inverted pyramid structures by photolithography masking, except that the mask used in photolithography was replaced by the  $\text{Na}_2\text{SiO}_3$  produced during the alkaline etching process because  $\text{Na}_2\text{SiO}_3$  is insoluble in EGBE. The mechanism is shown in Fig. 5. After  $\text{Na}_2\text{SiO}_3$  formed the mask, the  $\text{OH}^-$  groups continued to etch along the exposed silicon surface, and finally,  $\text{Na}_2\text{SiO}_3$  was deposited at the bottoms of the inverted pyramids, as shown in Fig. 6. The addition of sodium hydroxide (NaOH) solution results in a higher etch rate and better anisotropy between the (100) and (111) crystallographic planes. The silicon atoms on Si(100) plane are etched away at a faster rate compared to those on Si(111) plane, leading to the formation of a pyramidal structure. In other wet etching solutions, such as IPA (isopropyl alcohol), TMAH water solution, oxidation agents (e.g., ferricyanide  $\text{K}_3\text{Fe}(\text{CN})_6$ ), anionic SDSS(sodiumdioleyl

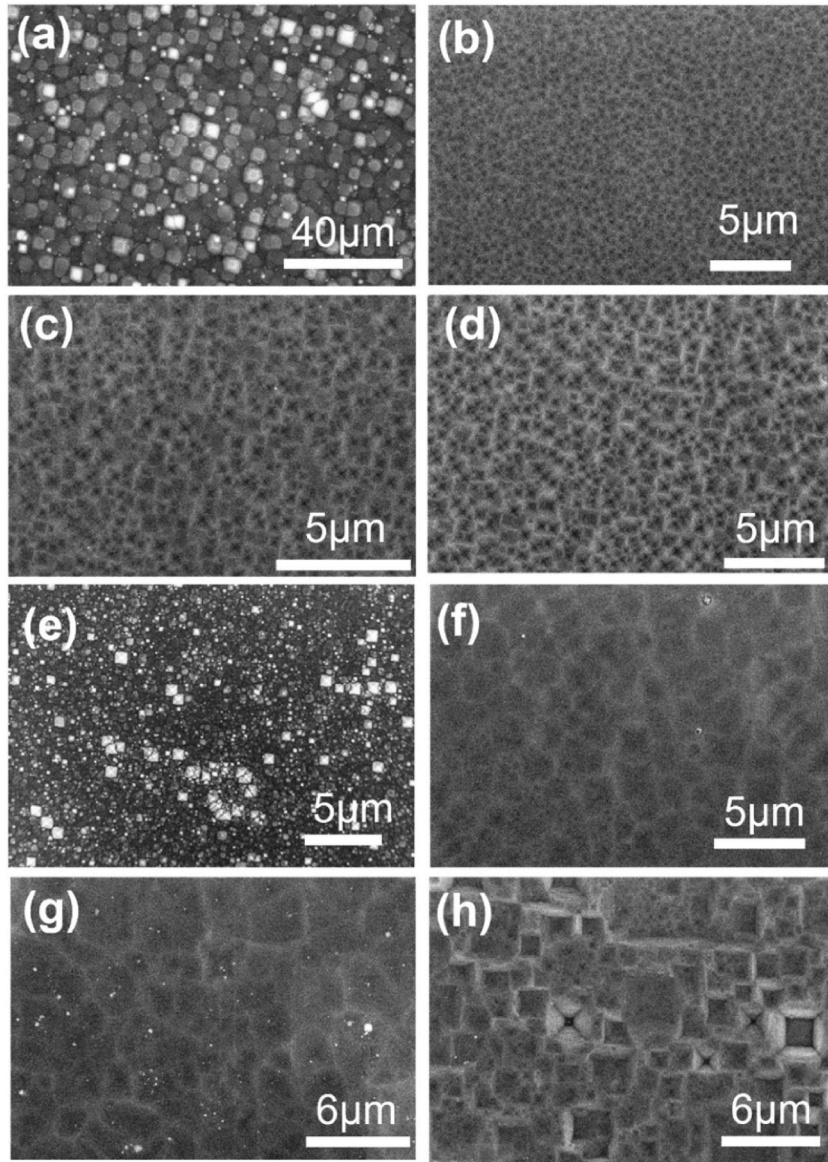
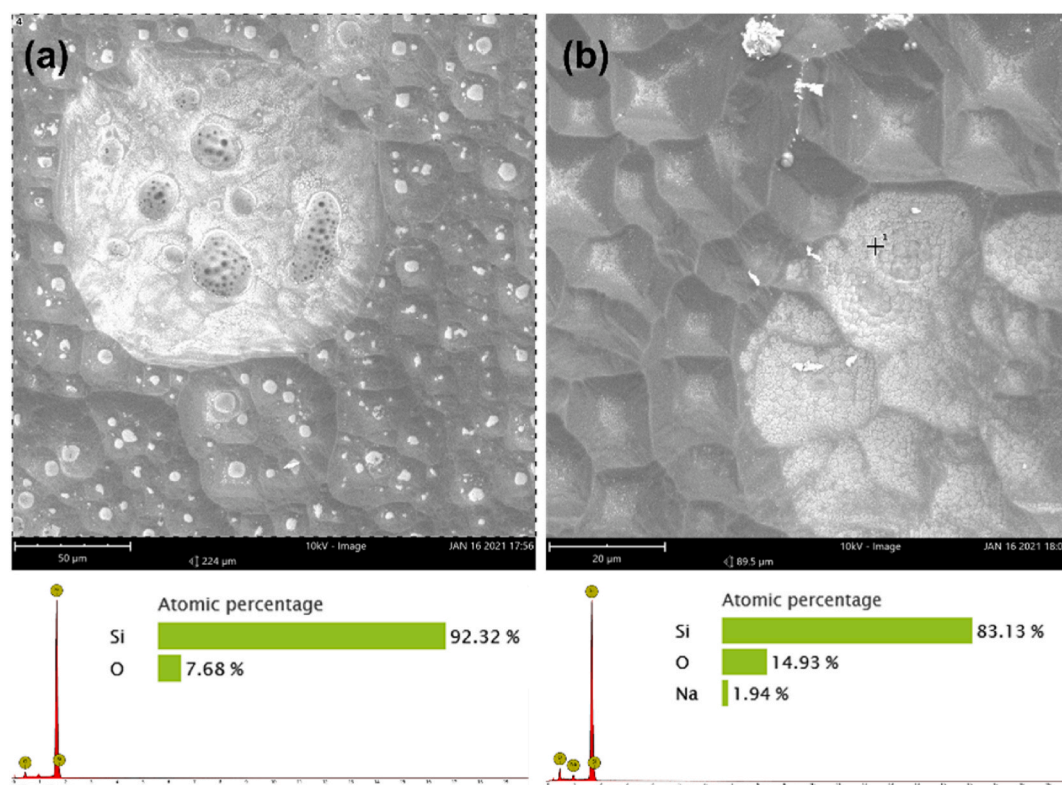


**Fig. 3.** SEM images showing the morphological evolution of inverted pyramid structures prepared by etching a p-type silicon wafer (B doped, 15–25  $\Omega \cdot \text{cm}$ , crystal direction (100)) in alkaline solutions with different EGBE concentrations and etching times; (a)–(d) 0.5 h; (e)–(h) 1 h.

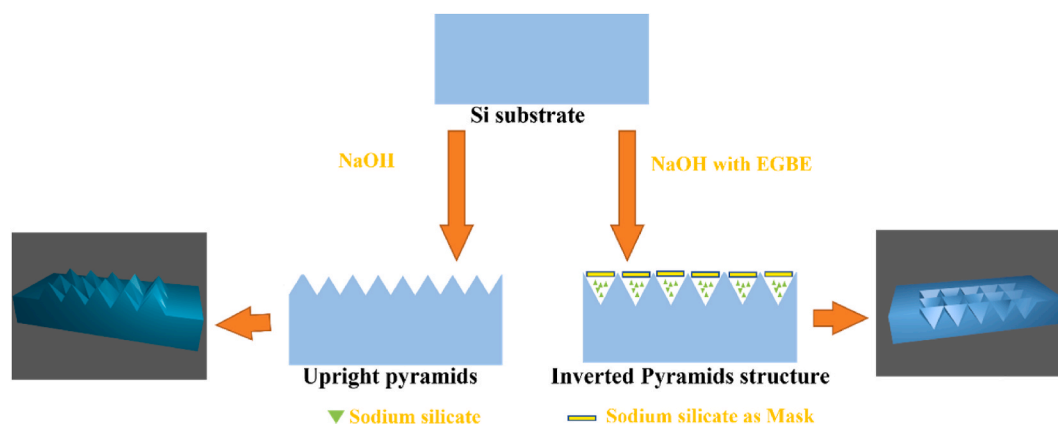
sulfosuccinate), cationic ASPEG (Acrylic polyethers), and non-ionic PEG (Polyethylene glycol)), the additives primarily serve to eliminate bubbles or accelerate the reaction process [44–46]. They do not alter the results obtained with sodium hydroxide and cannot change the upright pyramids into inverted pyramids. The role of EGBE is distinct from other reported additives. Its main function is to inhibit the dissolution of sodium silicate, allowing it to accumulate on the sites where silicon has already been etched by sodium hydroxide. This protects the underlying silicon from further reaction with sodium hydroxide. As sodium silicate accumulates on these sites, combined with the different atomic structures on the (100) and (111) surfaces of silicon, it becomes more difficult for the (111) surface to be etched, resulting in the formation of an initial inverted pyramid structure. Sodium silicate then deposits downward, and when all exposed silicon crystal faces are (111), it ultimately leads to the formation of an inverted pyramid structure.

Fig. 6(d) shows that when the silicon wafer was not cleaned after alkaline etching, the white substance, which was the  $\text{Na}_2\text{SiO}_3$  produced during the etching process, remained on the silicon surface. When we removed the etched silicon wafer from the PTFE reactor after the experiment, a white viscous substance adhered to the surface of the silicon wafer. After placing the silicon wafer in water, the white viscous substance immediately dissolved. In this system used for the NaOH and Si reaction, the only nongaseous product was  $\text{Na}_2\text{SiO}_3$ , and the reaction was as follows [23]:





**Fig. 4.** Surface EDS results obtained after etching silicon wafers with an alkaline mixed solution of EGBE and NaOH. (a) EDS scans of the whole surface region in the SEM image. (b) EDS spot scanning at the cross spot. (For interpretation of the references to colour in this figure legend, the reader is referred to the Web version of this article.)



**Fig. 5.** Schematic diagrams of conventional alkali etching to form an upright pyramid structure (left) and the use of EGBE to regulate the etching of silicon wafers by a NaOH solution to form an inverted pyramid structure (right). (For interpretation of the references to colour in this figure legend, the reader is referred to the Web version of this article.)

In summary, this study shows that the inverted pyramid structures can be produced on silicon surface with an alkaline solution containing EGBE. During etching, the  $\text{Na}_2\text{SiO}_3$  and EGBE played important roles. Silicon reacted with the alkaline solution of EGBE and NaOH to generate  $\text{Na}_2\text{SiO}_3$ , which deposited on the silicon surface to form a natural mask. Eventually, inverted pyramid structures were produced on the silicon surface. This method is applicable to any monocrystalline silicon wafer, as shown in Fig. 7. Fig. 7 provides SEM images of the inverted pyramid structures formed during alkaline etching of different types of silicon wafers: (a)-(b) show p-type polished silicon wafers (B-doped, 15–25  $\Omega\cdot\text{cm}$ , (100)), (c)-(d) show p-type silicon wafers sliced with a diamond wire (B-doped, 1–2  $\Omega\cdot\text{cm}$ , (100)), (e)-(f) show n-type polished silicon wafers (p-doped, 2–2.7  $\Omega\cdot\text{cm}$ , (100)), and (g)-(h) show p-type polycrystalline silicon



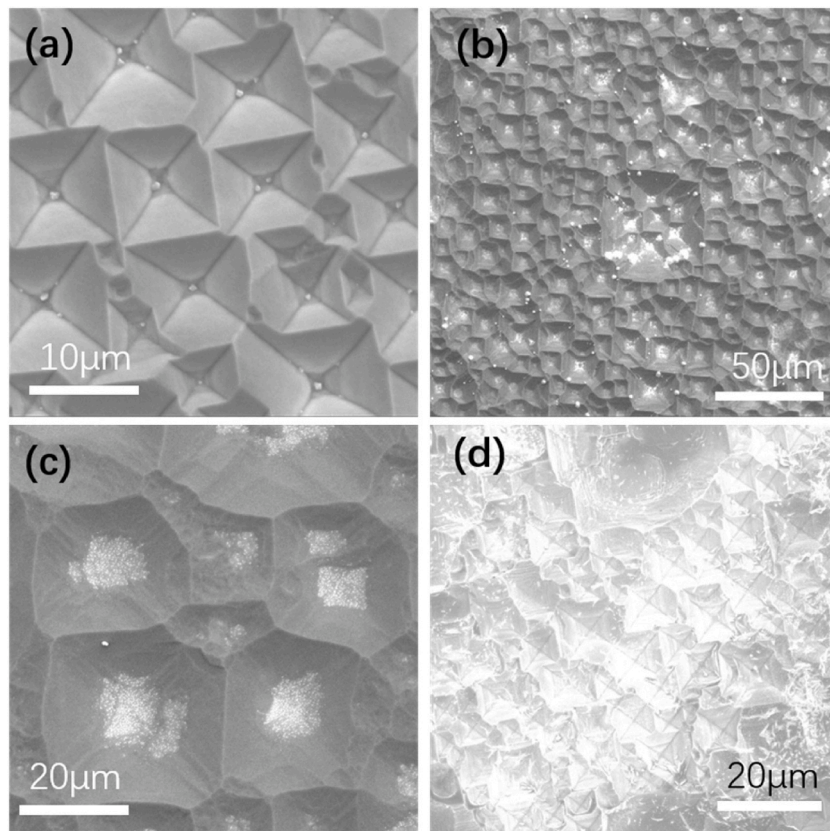


**Fig. 6.** SEM images of the p-type silicon wafer (B doped, 15–25  $\Omega \cdot \text{cm}$ , (100)) formed by etching with an alkaline mixed solution of EGBE and NaOH. The silicon wafer was not ultrasonically cleaned in (d).

wafers cut with a diamond wire (B-doped, 1–2  $\Omega \cdot \text{cm}$ ). When the silicon wafer exhibited a (100) crystal orientation, this method etched inverted pyramid structures on the surface of the silicon wafer. Silicon wafers with other crystalline orientations were etched to form triangular pit structures, as shown in Fig. 7(g)–(h).

As mentioned above, EGBE mixed with NaOH in an alkaline solution reacted with silicon to generate  $\text{Na}_2\text{SiO}_3$ , which deposited on the silicon surface to form a natural mask, and finally, inverted pyramid structures were formed on the silicon surface. This study employed the quality loss method to determine the reaction rate for silicon wafer etching by measuring the quality loss after a reaction time of 30 min and dividing it by the density and surface area of the silicon wafer to obtain the radial thickness reduction caused by etching. The results are shown in Fig. 8. As the total reaction time was increased, the average etching rate gradually decreased. This result is easy to understand because at first, all orientations were (100), and the etching rate was faster than those for other orientations. In the initial reaction stage, the silicon wafer lost more weight, indicating that the reaction was faster [18,23]. This study of the experiment and the relevant experimental phenomena showed that a polished silicon wafer with a thickness of approximately 500  $\mu\text{m}$  was completely etched away by the alkaline etchant within 6–9 h. With increasing reaction time, inverted pyramid structures gradually formed on the silicon surface, as shown in Fig. 9. Fig. 9 shows SEM images from the initial stage of the alkaline etching reaction with 45 ml EGBE and 1 % NaOH (mass fraction). The reaction times for Fig. 9 (a)–(d) were 1 min, 4 min, 12 min, and 15 min, respectively. From the time evolution results, when the etching time was 1 min, there were already very small pits formed on the silicon surface, and when the reaction time was increased to 4–12 min, the inverted pyramid structures were formed. When the reaction continued for approximately 15 min, the inverted pyramid structures became more regular.

Based on the experiments described in this work, we tested the reflectivity of the inverted pyramid structures, as shown in Fig. 10. The reflectivity results showed that both the upright and inverted pyramid structures increased the light absorption, resulting in a significant decrease in reflectivity [47,48]. The upright pyramid structures used in this experiment were prepared by mixing NaOH with a commercially available mono crystal solution, and the reflectivity was approximately 10 %. Compared with the upright pyramid structures, the reflectivity of the alkaline-etched inverted pyramid structures was similar for visible light but lower for light with short and long wavelengths of 200–1000 nm. Compared to other methods of preparing inverted pyramid structures, the biggest advantage of alkaline etching is its low cost, NaOH and EGBE are inexpensive, and the reaction products are nontoxic and do not pollute the air or environment. This differs from the  $\text{HF-HNO}_3$  acidic system, which generates toxic NOx gases that pollute the environment.

The entire fabrication process of the solar cells created in this study is shown in Fig. 11. The I–V characteristic curves of the solar cells are shown in Fig. 12. Curves were fabricated on a mono-crystalline silicon wafer with the proposed etching method. As shown in

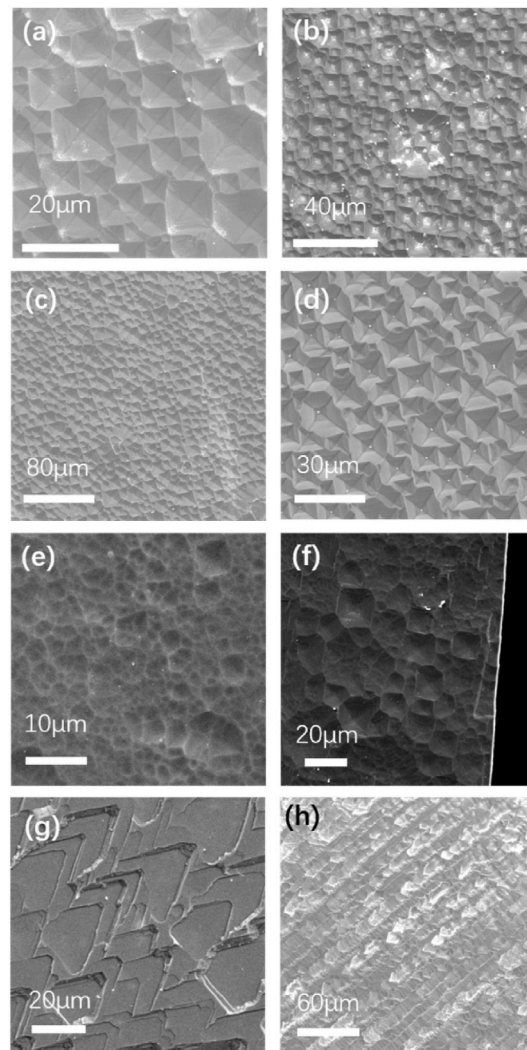


**Fig. 7.** SEM images of the inverted pyramid structures formed on different silicon wafers with an alkaline texturing solution; (a)–(b) p-type polished silicon wafer (B doped, 15–25  $\Omega\cdot\text{cm}$ , (100)), (c)–(d) p-type diamond wire-cut silicon wafer (B doped, 1–2  $\Omega\cdot\text{cm}$ , (100)), (e)–(f) N-type polished silicon wafer (p-doped, 2–2.7  $\Omega\cdot\text{cm}$ , (100)) and (g)–(h) p-type diamond wire-cut polysilicon wafer (B doped, 1–2  $\Omega\cdot\text{cm}$ ).

the curves, inverted pyramid structure solar cells prepared using PERC technology with the proposed texturing process have markedly high short-circuit current ( $I_{SC}$ ), open-circuit voltage ( $V_{OC}$ ) and fill factor ( $FF$ ). As shown in Table 3, the inverted pyramid structure was produced by NaOH with EGBE in 15min, the  $I_{SC}$ ,  $V_{OC}$ ,  $FF$  and  $\eta$  reached 0.67 V, 9.76 A, 80.74 and 21.54 %. The  $I_{SC}$  is higher because the inverted pyramid structure increases the reflection times of light on the front surface. The passivation layer on the rear after texturing also allowed more light to be absorbed on the rear electron field, thereby improving the cell efficiency [49,50].

The final finished cell is shown in Fig. 13(a). The solar cells prepared by the proposed texturing method appear dark black in appearance. The black silicon cells have lower reflectivity and thus effectively absorb more visible light, improving cell efficiency [51, 52]. Compared with Fig. 10 shows that the reflectivity of the prepared silicon wafer after the alkaline process is approximately 9 %. The reflectivity of the cell is less than 3 % after completing the entire cell process, as shown in blue lines of Fig. 13(b). The reflectance and IPCE (incident photon-to-electron conversion efficiency) characteristic values, including the internal quantum efficiency (IQE) and external quantum efficiency (EQE), of the mono-crystalline silicon solar cells prepared by the new alkaline method are shown in Fig. 13 (b). The IPCE diagram shows that the solar cell prepared by PERC technology achieves a high quantum efficiency. The reflectivity of the cell also decreased from 7 % after texturing to 2 % after the anti-reflection layer was deposited. Conversely, this material's low reflectivity is why the surface of the cell appears black. The IQE value of the cell was 94.95 % at 600 nm, which is a much higher value in the short wavelength range (450–600 nm), highlighting the excellent passivation ability of the antireflection layer and light trapping structure, which can reduce the recombination of the front surface of the cell [53]. The IQE value of 94.84 % at 800 nm in the mid- and long wavelength range (600–1000 nm) also indicates better light absorption near the P–N junction region, particularly the inverted pyramid effect at the front surface [49]. In the range of wavelengths greater than 1000 nm, the IQE value drops quickly because the



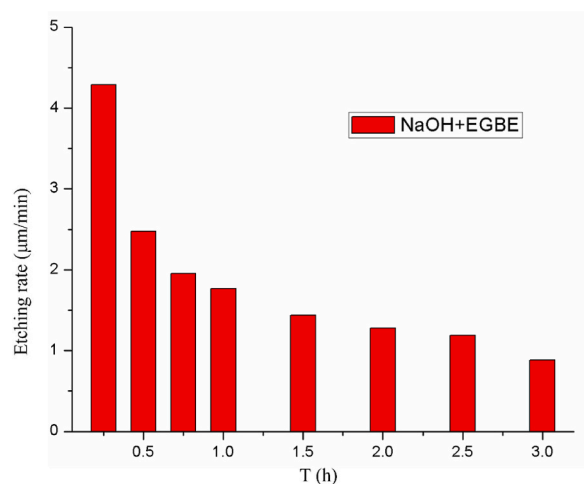


**Fig. 8.** Average etching rates for p-type silicon wafers (B doped, 15–25  $\Omega\cdot\text{cm}$ , (100)) in alkaline solution. (For interpretation of the references to colour in this figure legend, the reader is referred to the Web version of this article.)

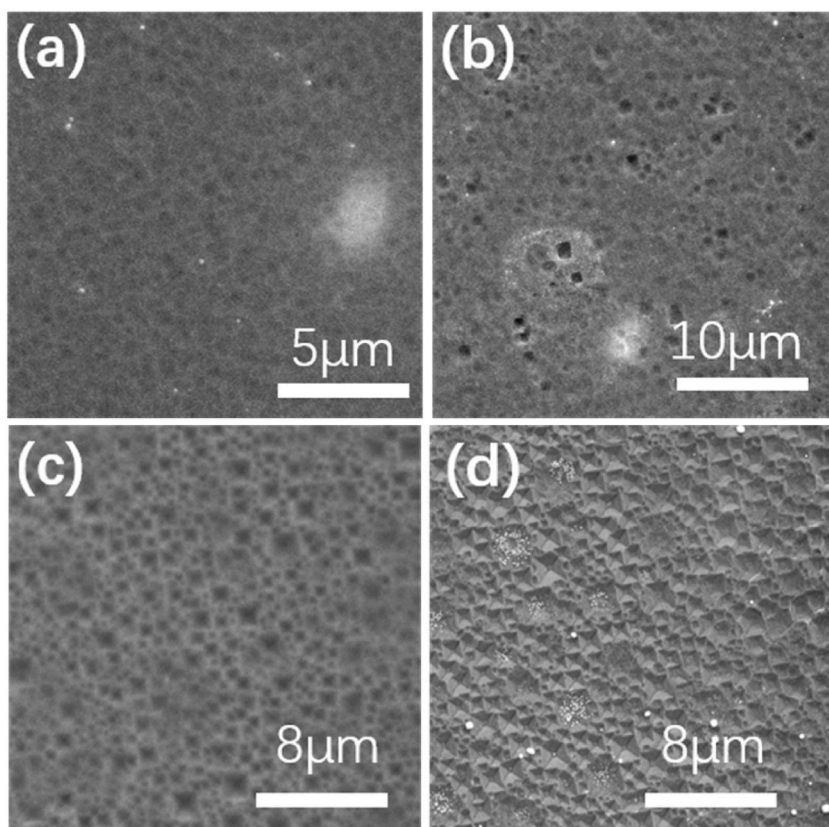


**Fig. 9.** (a)–(d) SEM images showing the morphological evolution over time of inverted pyramids prepared during etching of a p-type polished silicon wafer (B doped, 15–25  $\Omega\cdot\text{cm}$ , crystal direction is (100)) with 45 ml of a solution with EGBE and 1 % NaOH (mass fraction).

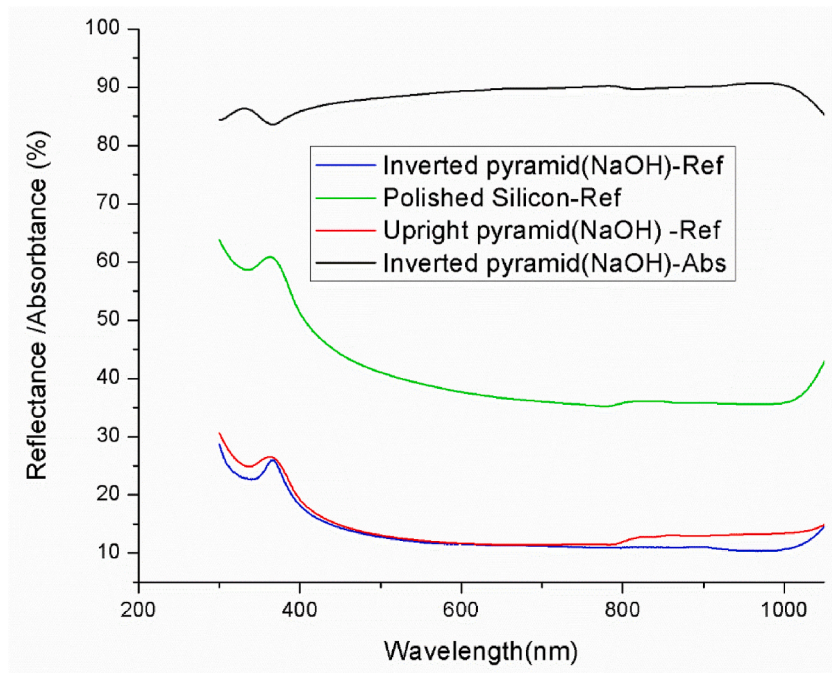


**Fig. 10.** Reflectivity and absorption comparison for the inverted pyramid structure prepared by EGBE and NaOH with conventional upright pyramid structures and a flat polished silicon wafer. (For interpretation of the references to colour in this figure legend, the reader is referred to the Web version of this article.)

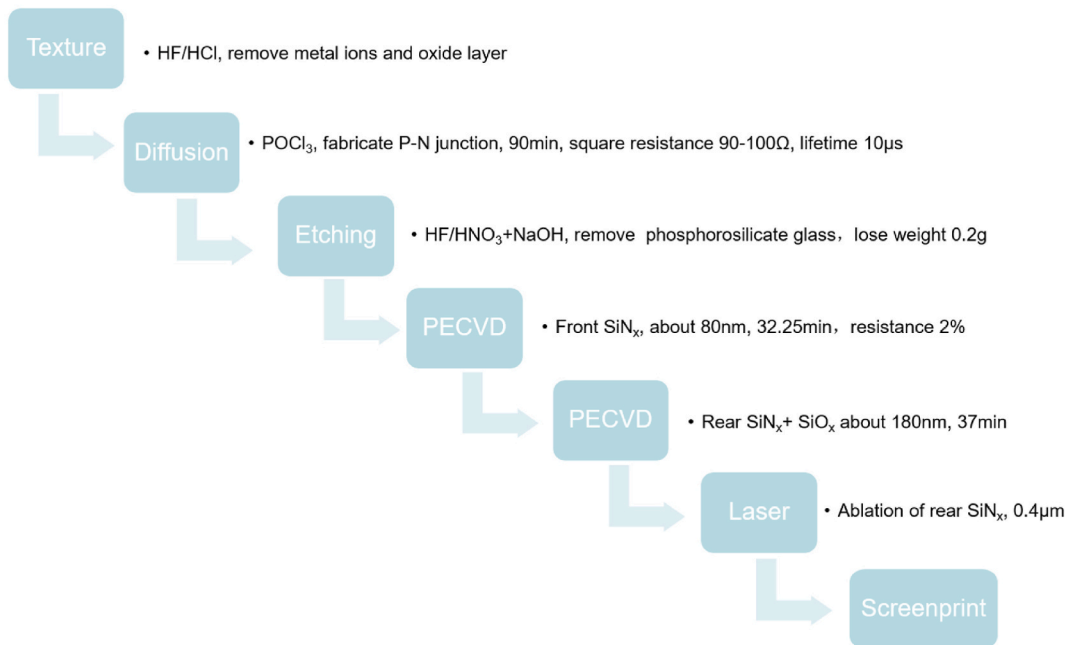


**Fig. 11.** Schematic diagram of preparing mono-crystalline silicon solar cell. (For interpretation of the references to colour in this figure legend, the reader is referred to the Web version of this article.)

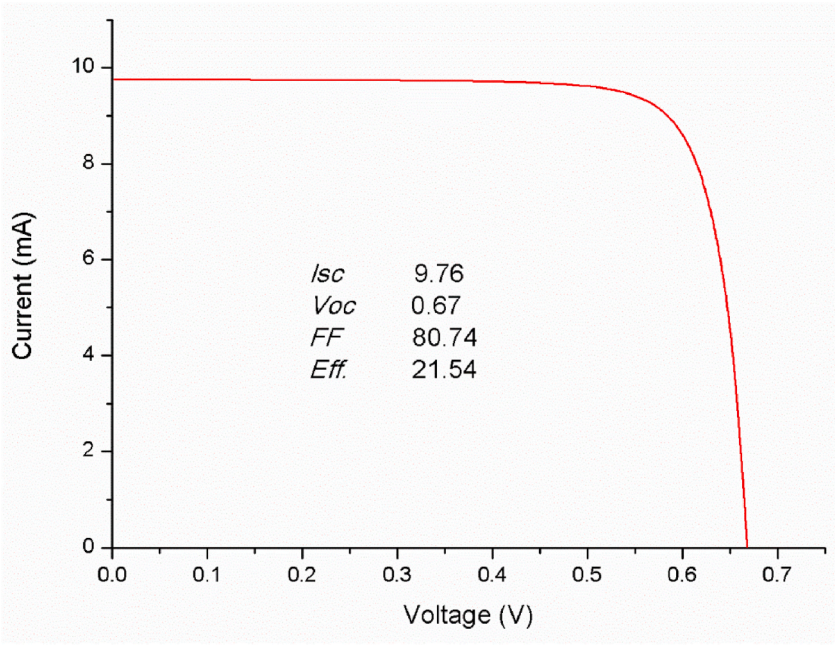


**Fig. 12.** I–V characteristic curves of silicon solar cell with inverted pyramid structures. (For interpretation of the references to colour in this figure legend, the reader is referred to the Web version of this article.)

**Table 3**  
Efficiency of crystalline silicon solar cell with inverted pyramid structure.

Etching time (min)	$I_{sc}$ (A)	$V_{oc}$ (V)	$FF$ (%)	$\eta$ (%)
15min	9.76	0.67	80.74	21.54

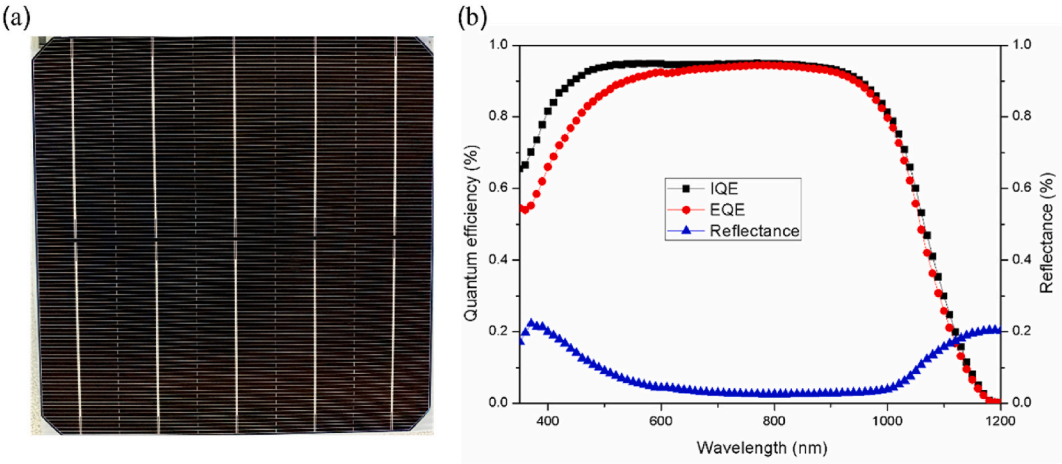


**Fig. 13.** (a) Photo of mono-crystalline silicon solar cell with inverted pyramid structure. (b) IPCE spectra of mono-crystalline silicon solar cell with new texturing. (For interpretation of the references to colour in this figure legend, the reader is referred to the Web version of this article.)

energy gap limitation of the *P*-type silicon wafer cannot absorb the energy of long-wavelength photons. Overall, the texture of the inverted pyramid has a strong effect on the absorption of photons near visible light wavelengths.

#### 4. Conclusion

Inverted pyramid structures were successfully prepared on silicon surfaces with alkaline solutions. This experimental method was the first to use a one-step alkaline etching method to etch inverted pyramids on a monocrystalline silicon wafer. The inverted pyramid structures prepared by alkaline etching showed regular shapes and sizes that met the requirements for silicon solar cells. This method can be applied to different types of polished or diamond wire-cut silicon wafers. Based on many experiments, we proposed a mechanism for preparing inverted pyramid structures by alkaline etching. We believe that the added EGBE blocked the dissolution of  $\text{Na}_2\text{SiO}_3$  during the alkaline etching process, which caused the  $\text{Na}_2\text{SiO}_3$  to deposit on the silicon surface and act as a mask. Combined with alkaline anisotropic etching, this led to the formation of inverted pyramid structures. Additionally, this paper provides a mechanistic explanation for the preparation of inverted pyramids by alkaline etching. After etching, some white solid remained on the silicon surface, which quickly dissolved when placed in water. Based on the alkaline etching process and the EDS element analyses, it is believed that the white solid was  $\text{Na}_2\text{SiO}_3$ , which is the only product from alkaline etching other than water. Because  $\text{Na}_2\text{SiO}_3$  became saturated in the water and is insoluble in EGBE, it precipitated on the silicon surface and acted as lithography masks, allowing hydroxide to etch the uncoated areas of the silicon surface and thus form the inverted pyramid structures, as in photolithography. The inverted pyramid structures prepared by alkaline etching exhibited a lower reflectivity than the conventional upright pyramid structure and flat polished silicon wafer. In addition, we fabricated mono-crystalline silicon solar cells with inverted pyramid structures using this method. The resulting cells exhibited an efficiency of 21.54 %, illustrating the applicability of this alkaline etching-based inverted pyramid fabrication method in solar cell manufacturing.

Although inverted pyramid structures were first prepared via a one-step method in alkaline solutions, the mechanism still needs further study, and more research is needed to find other low-cost materials or more universal solution methods.

#### Funding

We gratefully acknowledge the financial support from National Natural Science Foundation of China (51972031, 52371210), Beijing Municipal Natural Science Foundation.

#### Data availability statement

Data will be made available on request.

#### CRediT authorship contribution statement

**Chenliang Huo:** Writing – review & editing, Writing – original draft, Methodology, Data curation. **Haoxin Fu:** Data curation. **Kui-Qing Peng:** Writing – review & editing, Project administration, Funding acquisition, Conceptualization.

#### Declaration of competing interest

The authors declare that they have no known competing financial interests or personal relationships that could have appeared to influence the work reported in this paper.

#### References

- [1] G. Adolf, L. Joachim, W. Gerhard, Solar cells: past, present, future, 2002 *Solar Energy Materials and Solar Cells* 74 (2002) 1–11.
- [2] H. Fang, K. Yu, et al., Capacitively coupled arrays of multiplexed flexible silicon transistors for long-term cardiac electrophysiology, *Nat. Biomed. Eng.* 1 (2017) 38.
- [3] Y. Jiang, J. Carvalho-de-Souza, et al., Heterogeneous silicon mesostructures for lipid-supported bioelectric interfaces, *Nat. Mater.* 15 (2016) 1023–1030.
- [4] M. Rodrigues, G. Babu, et al., A materials perspective on Li-ion batteries at extreme temperatures, *Nat. Energy* 2 (2017), 17108.
- [5] J. Zhuang, X. Xu, G. Peleckis, W. Hao, S.X. Dou, Y. Du, Silicene: a promising anode for lithium-ion batteries, *Adv. Mater.* 29 (2017), 1606716.
- [6] M. Green, S. Bremner, Energy conversion approaches and materials for high-efficiency photovoltaics, *Nat. Mater.* 16 (2017) 23–24.
- [7] B. Min, M. Muller, et al., A roadmap toward 24% efficient PERC solar cells in industrial mass production, *IEEE J. Photovoltaics* 7 (2017) 1541–1550.
- [8] H. Huang, J. Lv, et al., 20.8% industrial PERC solar cell: ALD  $\text{Al}_2\text{O}_3$  rear surface passivation, efficiency loss mechanisms analysis and roadmap to 24, *Sol. Energy Mater. Sol. Cell.* 161 (2017) 14–30.
- [9] C. Huo, J. Wang, H. Fu, et al., Metal-assisted chemical etching of silicon in oxidizing HF solutions: origin, mechanism, development, and black silicon solar cell application, *Adv. Funct. Mater.* 30 (2020), 2005744.
- [10] K. Peng, Y. Yan, et al., Synthesis of large-area silicon nanowire arrays via self-assembling nanoelectrochemistry, *Adv. Mater.* 14 (2002) 1164–1167.
- [11] Hiroyuki Kanda, Uzum, Abdullah, Harano, et al.,  $\text{Al}_2\text{O}_3/\text{TiO}_2$  double layer anti-reflection coating film for crystalline silicon solar cells formed by spray pyrolysis, *Energy Sci. Eng.* 4 (2016) 269–276.
- [12] A. Jörg, R. Anja, et al., Mass and electron balance for the oxidation of silicon during the wet chemical etching in  $\text{HF}/\text{HNO}_3$  mixtures, *J. Phys. Chem. C* 116 (2012) 20380–20388.
- [13] E. Vazsonyi, K. De Clercq, et al., Improved anisotropic etching process for industrial texturing of silicon solar cells, *Sol. Energy Mater. Sol. Cell.* 57 (1999) 179–188.
- [14] F. Huang, B. Guo, et al., Plasma-produced ZnO nanorod arrays as an antireflective layer in c-Si solar cells, *J. Mater. Sci.* 54 (2019) 4011–4023.



- [15] C. Bian, B. Zhang, et al., Wafer-scale fabrication of silicon nanocones via controlling catalyst evolution in all-wet metal-assisted chemical etching, *ACS Omega* 7 (2022) 2234–2243.
- [16] Z.Y. Yeo, Z.P. Ling, et al., Status review and future perspectives on mitigating light-induced degradation on silicon-based solar cells, *Renew. Sustain. Energy Rev.* 159 (2022), 112223.
- [17] D. Chapin, C. Fuller, et al., A new silicon p-n junction photocell for converting solar radiation into electrical power, *J. Appl. Phys.* 25 (1954) 676–677.
- [18] H. Seidel, L. Csepregi, A. Heuberger, et al., Anisotropic etching of crystalline silicon in alkaline solutions I. orientation dependence and behavior of passivation layers, *J. Electrochem. Soc.* 137 (1990) 3612–3626.
- [19] H. Seidel, L. Csepregi, A. Heuberger, et al., Anisotropic etching of crystalline silicon in alkaline solutions II. influence of dopants, *J. Electrochem. Soc.* 137 (1990) 3626–3632.
- [20] S. Joong, et al., Effect of temperature on the interaction of silicon with nonionic surfactants in alkaline solutions, *J. Electrochem. Soc.* 143 (1996) 277.
- [21] N.A. Chuchvaga, N.M. Kislyakova, et al., Problems arising from using KOH-IPA etchant to texture silicon wafers, *Tech. Phys.* 65 (2020) 1685–1689.
- [22] F. Yujie, H. Peide, et al., Differences in etching characteristics of TMAH and KOH on preparing inverted pyramids for silicon solar cells, *Appl. Surf. Sci.* 264 (2013) 761–766.
- [23] P. Allongue, et al., Etching of silicon in NaOH solutions: II. Electrochemical studies of n-Si(111) and (100) and mechanism of the dissolution, *J. Electrochem. Soc.* 140 (1993) 1018.
- [24] S. Kaoru, et al., Etching characteristics of Si(100) surfaces in an aqueous NaOH solution, *J. Electrochem. Soc.* 147 (2000) 1530.
- [25] V. Quoc-Bao, et al., Surface characteristics of (100) silicon anisotropically etched in aqueous KOH, *J. Electrochem. Soc.* 143 (1996) 1372.
- [26] J. Zhao, A. Wang, et al., 24% efficient perl silicon solar cell: recent improvements in high efficiency silicon cell research, *Sol. Energy Mater. Sol. Cell.* 42 (1996) 87–99.
- [27] J. Zhao, A. Wang, M. Green, 24% efficient PERL structure silicon solar cells, *Photovoltaic Specialists Conference, Confer. Record of the Twenty First IEEE* 1 (1990) (2002) 333.
- [28] M. Green, J. Zhao, et al., Progress and outlook for high-efficiency crystalline silicon solar cells, *Sol. Energy Mater. Sol. Cell.* 65 (2001) 9–16.
- [29] M. Green, The passivated emitter and rear cell (PERC) from conception to mass production, *Sol. Energy Mater. Sol. Cell.* 143 (2005) 190–197.
- [30] K.Q. Peng, A.J. Lu, et al., Motility of metal nanoparticles in silicon and induced anisotropic silicon etching, *Adv. Funct. Mater.* 18 (2008) 3026–3035.
- [31] X. Wang, K.Q. Peng, et al., Silicon/hematite core/shell nanowire array decorated with gold nanoparticles for unbiased solar water oxidation, *Nano Lett.* 14 (2014) 18–23.
- [32] J. Wang, Y. Hu, et al., Oxidant concentration modulated metal/silicon interface electrical field mediates metal-assisted chemical etching of silicon, *Adv. Mater. Interfac.* 5 (2018), 1801132.
- [33] C. Huo, J. Wang, et al., Metal-assisted chemical etching of silicon: origin, mechanism, and black silicon solar cell applications, in: M.F. Müller (Ed.), *Photovoltaic Manufacturing*, 2021, pp. 1–36.
- [34] K. Ding, M. Zhang, et al., High-resolution image patterned silicon wafer with inverted pyramid micro-structure arrays for decorative solar cells, *Mater. Today Energy* 18 (2020), 100493.
- [35] K. Tsujino, M. Matsumura, Y. Nishimoto, Texturization of multicrystalline silicon wafers for solar cells by chemical treatment using metallic catalyst, *Sol. Energy Mater. Sol. Cell.* 90 (2006) 100–110.
- [36] X. Ye, S. Zou, et al., 18.45%-Efficient multi-crystalline silicon solar cells with novel nanoscale pseudo-pyramid texture, *Adv. Funct. Mater.* 24 (2014) 6708–6716.
- [37] X. Lin, Y. Zeng, et al., Realization of improved efficiency on nanostructured multicrystalline silicon solar cells for mass production, *Nanotechnology* 26 (2015), 125401.
- [38] H. Xu, S. Zhong, et al., Controllable nanoscale inverted pyramids for highly efficient quasi-omnidirectional crystalline silicon solar cells, *Nanotechnology* 29 (2018), 015403.
- [39] C. Lai, X. Li, et al., Study on corrosion of porous silicon in KOH and NaOH solution, *Corrosion Engineering, Sci. Technol.* 49 (2014) 386–389.
- [40] C.L. Guo, R. Jia, X.R. Tian, et al., Study on the influence of micro-alkali texturing and micro-alkali polishing process on the passivation and contact performance of n-TOPCon solar cells, *Sol. Energy Mater. Sol. Cell.* 260 (2023), 112476.
- [41] Y. Wang, Y. Liu, et al., Micro-structured inverted pyramid texturization of Si inspired by self-assembled Cu nanoparticles, *Nanoscale* 9 (2017) 907–914.
- [42] A. Srivastava, D. Sharma, et al., Excellent omnidirectional light trapping properties of inverted micro-pyramid structured silicon by copper catalyzed chemical etching, *Opt. Mater.* 131 (2022), 112677.
- [43] A. Miguel, I. Gosálvez, et al., Chapter 17 - wet etching of silicon, in: Markku Tili, et al. (Eds.), *Micro and Nano Technologies, Handbook of Silicon Based MEMS Materials and Technologies*, third ed., Elsevier, 2010, pp. 447–480.
- [44] C. Moldovan, R. Iosub, et al., Anisotropic etching of silicon in a complexant redox alkaline system, *Sensor. Actuator. B Chem.* 58 (1999) 438–449.
- [45] V. Swarnalatha, P. Pal, Effective improvement in the etching characteristics of Si(110) in low concentration TMAH solution, *Micro & Nano Lett.* 13 (2018) 1085–1089.
- [46] P. Pal, V. Swarnalatha, A.V.N. Rao, et al., High speed silicon wet anisotropic etching for applications in bulk micromachining: a review, *Micro and Nano Syst. Lett.* 9 (2021) 4.
- [47] L. Yang, Y. Liu, et al., 18.87%-efficient inverted pyramid structured silicon solar cell by one-step Cu-assisted texturization technique, *Sol. Energy Mater. Sol. Cells* 166 (2017) 121–126.
- [48] S.C. Baker-Finch, K.R. McIntosh, Reflection of normally incident light from silicon solar cells with pyramidal texture, *Prog. Photovoltaics Res. Appl.* 19 (2011) 406–416.
- [49] D. Zhang, S. Jiang, et al., Fabrication of inverted pyramid structure for high-efficiency silicon solar cells using metal assisted chemical etching method with CuSO<sub>4</sub> etchant, *Sol. Energy Mater. Sol. Cell.* 15 (2021), 111200.
- [50] H. Tang, Y. Liu, Optical design of inverted pyramid textured PERC solar cells, *ACS Appl. Electron. Mater.* 1 (2019) 2684–2691.
- [51] J. Wu, Y. Liu, et al., Influence of different-sized inverted-pyramids of silicon texture by Ag manipulation on solar cell performance, *Appl. Surf. Sci.* 15 (2020), 144778.
- [52] R. Tong, C. Li, Upright pyramids vs. inverted pyramids surface textures: a comparative investigation on the electrical properties of PERC solar cells, *J. Mater. Sci. Mater. Electron.* 34 (2023) 54.
- [53] L. Andreani, A. Bozzola, et al., Silicon solar cells: toward the efficiency limits, *Adv. Phys. X* 4 (2019) 1.